Validation of Shock-Expansion Tool for Two-dimensional and Axisymmetric Flows with CFD

Jyothi Kumar Puttam Shankara Rao Gonti[1]
Computational & Theoretical Fluid Dynamics Division
Council of Scientific and Industrial Research - National Aerospace Laboratories
Bangalore - 560017, INDIA.
Corresponding author e-mail: *jyothi@ctfd.cmmacs.ernet.in*

Abstract

The paper discusses the development and testing of shock-expansion tool for 2-D and axisymmetric supersonic and hypersonic flows. The motivation is to compute the first-cut inviscid surface flow parameters on bodies with sharp leading edges and attached shocks in minimum possible time without the necessity of grid. The flow parameters on the body surface immediately behind the leading edge shock are computed using either by solving oblique shock relation(two-dimensional flows: plane shock case) or by solving Taylor-Maccoll equation (axisymmetric flows: conical shock case). The subsequent flow parameters are computed either by Prandtl-Meyer relation (for isentropic expansion) or again by oblique shock relation (for compression) depending upon local surface inclination. The transcendental equations come into picture, while solving oblique shock or Prandtl-Meyer relations are solved using bi-section method. The Taylor-Maccoll equation is a second order ODE and was solved using RK-4 method. In the present study shock-expansion tool was tested for three 2-D bodies at different angle of attacks and three axisymmetric bodies at different Mach numbers with zero angle of incidence. In almost all the cases the results are in good agreement with Euler results computed using in-house RANS solver MB-EURANIUM and predicted the trends of experimental ones.

Key words: Supersonic Flow, Hypersonic Flow, Inviscid analysis, Oblique shock, Prandtl-Meyer expansion, Bi-section method.

1 Introduction

In the very early stage of design cycle usage of some analytical tools helps in saving lot of time by filtering out some designs, which are unable meet the specification requirements, and thus eliminates detailed analysis on those. In supersonic and hypersonic vehicles design, inviscid flow analysis is one such option, which eliminates the computationally expensive and much time consuming viscous flow analysis, in the very early stage. For inviscid analysis of supersonic/hypersonic aerodynamic flows, shock-expansion method is one such tool, which falls in the class of local surface inclination methods, and computes the surface flow parameters [1]. In supersonic/hypersonic flows there are three families of characteristics, viz the outward-running Mach waves from the body surface, the inward-running Mach waves from the shock and stream lines. The shock-expansion method neglects the interaction of first family of characteristics with last two families and thus gives the surface flow parameters exactly, only when the neglected interactions are really negligible [2].

The surface flow parameters over two-dimensional or axisymmetric bodies with sharp leading edges and attached shocks can be predicted with shock-expansion method. The first step of shock-expansion method is to find the flow properties immediately behind the nose shock. For two-dimensional bodies(plane shock case), it can be accomplished by solving oblique shock relation, where as for axisymmetric bodies(conical shock case) the solution of Taylor-Maccoll equation is required. The subsequent flow parameters are computed either by Prandtl-Meyer relation (for isentropic expansion) or again by

[1]Project Student, Department of Aerospace Engineering, HAA, Marathahalli, Bangalore

oblique shock relation (for compression) depending upon local surface inclination.
The concept of shock-expansion theory was first used by Epstein [3] for determining the surface pressure of an airfoil behind a shock. This concept of surface pressure determination was extended by Eggers et al [4] for approximate determination of shock shape and entire flow field as "generalised shock-expansion method". Later Syvertson et al [5] extended generalised shock-expansion method to bodies of revolutions near zero lift as second-order shock-expansion method. Jackson et al [6] combined second-order shock-expansion theory with modified Newtonian theory to compute flow field on blunt nosed configuration with/without flares. Later DeJarnette et al [7] made lot of improvements to find exact pressure gradient expression downstream a corner and found a new technique to find surface pressures at different angle of incidence. Later real gas effects were also included with second-order shock-expansion method by Moore et al [8].
The aim of the present work is to develop and test shock-expansion tool. First it was tested on three 2-D bodies viz, 5% thick diamond airfoil, 10% thick bi-convex airfoil and center-line symmetric section contour of all-body hypersonic aircraft at different angle of attacks. Next the tool was tested on three axisymmetric bodies viz, cones with different semi-vertex angles, tangent-ogive cylinder with fineness ration of 3 and cone-cylinder-flare configuration at zero angle of incidence for different Mach numbers. In all the cases the results were compared with Euler results computed using in-house RANS solver MB-EURANIUM and available experimental results.

2 Shock-expansion tool: solution methodology

As said in introduction the flow should be supersonic/hypersonic on the entire surface to utilize shock-expansion method and the body should have a sharp pointed nose to hold an attached oblique shock either plane or conical one. Shock-expansion method consists of two steps. The first step is to determine the flow parameters immediately behind the nose shock either by solving oblique shock relation for plane shock case or by solving Taylor-Maccoll equation for conical shock case. The second step is to determine the subsequent flow parameters on entire surface either by solving Prandtl-Meyer relation for isentropic expansion fan case or by solving oblique shock relation for compression shock case, depending upon local surface inclination. The solution techniques used in the present work for solving each of the above equations is explained in the following sections.

2.1 Oblique shock relation

For a given free-stream Mach number, M the flow deflection angle, θ and oblique shock angle, β can be related with oblique shock relation as follows:

$$\tan\theta = 2\cot\beta\frac{M^2\sin^2\beta - 1}{M^2(\gamma + \cos 2\beta) + 2} \quad \ldots\ldots\ldots (1)$$

Equation 1 is called as θ-β-M relation, which is a transcendental equations and was solved using bi-section method.

2.2 Taylor-Maccoll equation

Inviscid conical supersonic flows, with the assumption of constant parameters along rays from apex, are governed by Taylor-Maccoll equation, which is a second order ODE and was solved using Range-Kutta

4^{th} order method through an inverse approach. In contrast to finding the shock angle for a given cone (direct approach), we assume a shock angle and find the semi-vertex angle of cone, which supports that shock. By iterating on shock angle with bi-section method, the shock angle of the given right circular cone can be approached.

2.3 Prandtl-Meyer relation

The isentropic expansion of supersonic flows are governed by Prandtl-Meyer relation, which is also a transcendental equations and was solved like oblique shock relation.

3 Results

3.1 Two-dimensional flows

In all two-dimensional test cases 200 equidistant points were considered on both upper and lower surface for shock-expansion tool, where as 400 X 50 cells O-grids were used for inviscid CFD analysis.

3.1.1 5% thick diamond airfoil

The tests were carried out at a free-stream Mach number of 6.86 and at 0°, 5°, 10°, 15° and 20° angle of attacks. Figure 1(a) shows the Euler grid used for inviscid CFD analysis, where as figure 1(b) shows pressure contours with streamlines around diamond airfoil at 20° angle of attack. The experimental results of McLellan et al [9] were used for comparison, which were conducted at Langley 11-inch hypersonic tunnel at Reynolds number of $0.98X10^6$. Figure 2 shows the comparison of pressure coefficient ($(P - P_\infty)/P_\infty$) between Shock-expansion, experimental and Euler CFD results at different angle of attacks. It can be seen that there is good agreement between shock-expansion and Euler CFD results. But they over predicted compared to experimental results on suction side and the deviation increased with angle of attack, which can be attributed to increasing viscous effects with angle of attack, where as there is very good agreement on pressure side between all three sets of results.

3.1.2 10% thick bi-convex airfoil

The tests were carried out at a free-stream Mach number of 6.86 and at 0°, 6°, 10°, 15° and 20° angle of attacks. Figure 3(a) shows the Euler grid used for inviscid CFD analysis and figure 3(b) shows pressure contours with streamlines around bi-convex airfoil at 20° angle of attack. The experimental results of McLellan et al [9] were used for comparison, which were conducted at Langley 11-inch hypersonic tunnel at Reynolds number of $0.98X10^6$. Figure 4 shows the comparison of pressure coefficient ($(P - P_\infty)/P_\infty$) between Shock-expansion, experimental and Euler CFD results at different angle of attacks. Bi-convex airfoil results have exhibited very much similar behaviour of diamond airfoil.

3.1.3 All-body hypersonic aircraft pitch plane contour

All-body hypersonic aircraft model is representative of a hypersonic cruise vehicle, which was used to establish benchmark experimental data base for validation of advanced CFD codes. The experiments were conducted at NASA Ames 3.5-foot Hypersonic Wind Tunnel by Lockman et al [10].In the present study, the pitch plane symmetric section surface contour of all-body hypersonic aircraft was used as a

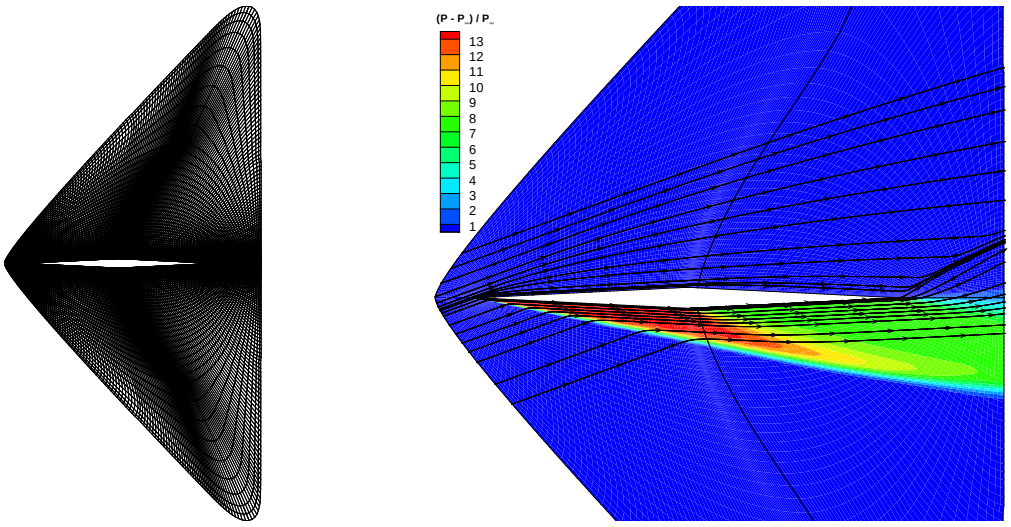

(a) Euler grid around diamond airfoil (b) Pressure contours with streamlines at aoa = 20°

Figure 1: Euler grid and pressure contours on 5% thick diamond airfoil at free-stream Mach number of 6.86 and 20° angle of attack

2-D test case for shock-expansion tool, to test at a free-stream Mach number of 7.4 and at 0°, 5°, 10° and 15° angle of attacks. Figure 5(a) shows the Euler grid used for inviscid CFD analysis and figure 5(b) shows pressure contours with streamlines around all-body hypersonic aircraft pitch plane contour at 15° angle of attack. The same experimental results of Lockman et al [10] were used for comparison, which were conducted at Reynolds number of $15X10^{6}$. Figures 5 (c) and (d) shows the comparison of pressure coefficient (P/P_{∞}) between shock-expansion, experimental and Euler CFD results at different angle of attacks respectively on leeward and windward sides of all-body hypersonic aircraft pitch plane contour. Like in the previous cases shock-expansion and Euler CFD results are in very good agreement on both suction and pressure sides, where as they underpredicted on suction side. On pressure side inviscid results overpredicted from experimental ones and the deviation increased with angle of attack, but within 9% band at maximum angle of attack of 15°.

3.2 Axisymmetric flows

In all axisymmetric test cases 200 equidistant points were considered on body surface for shock-expansion tool, where as 200 X 75 X 32 cells grids were used over half-body for inviscid CFD analysis.

3.2.1 Cones with different semi-vertex angles

Right circular cones with semi-vertex angles of 10°, 15° and 20° were used to test at a free-stream Mach number of 2.72. Figure 6(a) shows the Euler grid used for inviscid CFD analysis and figure 6(b) shows pressure contours with streamlines on right circular cone with semi-vertex angle of 20°. The experimental results of Yaholam [11] were used for comparison purpose, which were conducted at Reynolds number of $5.5X10^{5}$. Table 1 shows the comparison of C_p between shock-expansion, experimental and Euler CFD results for different right circular cones considered. Shock-expansion results underpredicted,

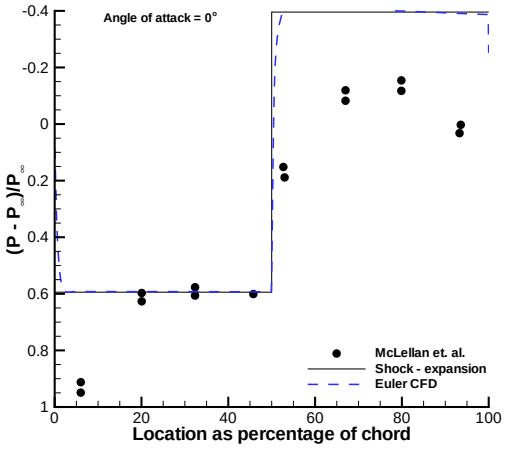

(a) Pressure distribution at aoa = 0°

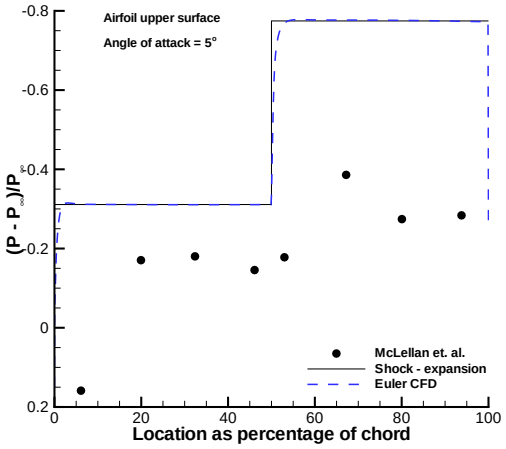

(b) Upper surface pressure distribution at aoa = 5°

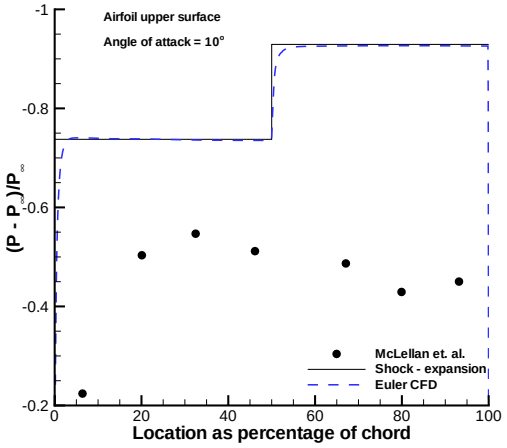

(c) Upper surface pressure distribution at aoa = 10°

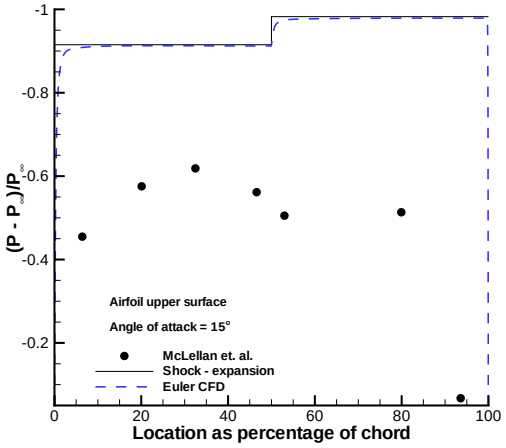

(d) Upper surface pressure distribution at aoa = 15°

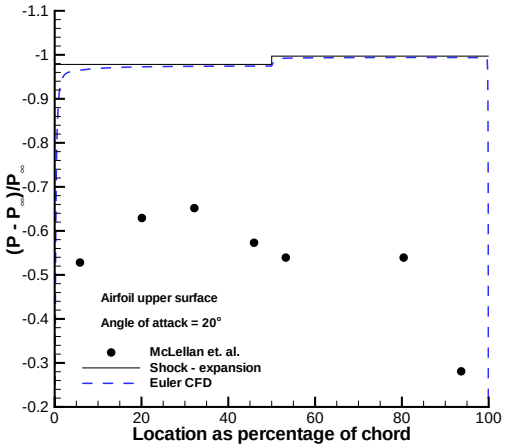

(e) Upper surface pressure distribution at aoa = 20°

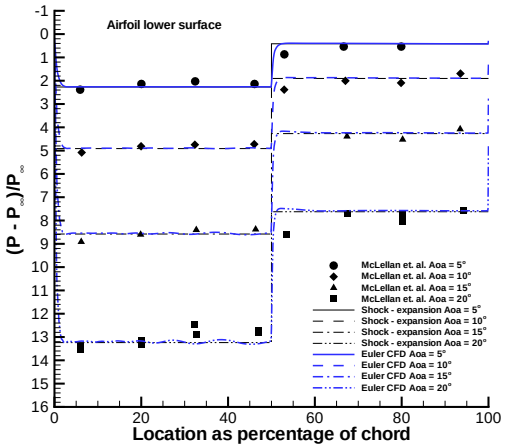

(f) Lower surface pressure distribution

Figure 2: Pressure distribution on 5% thick diamond airfoil at free-stream Mach number of 6.86 and different angle of attacks

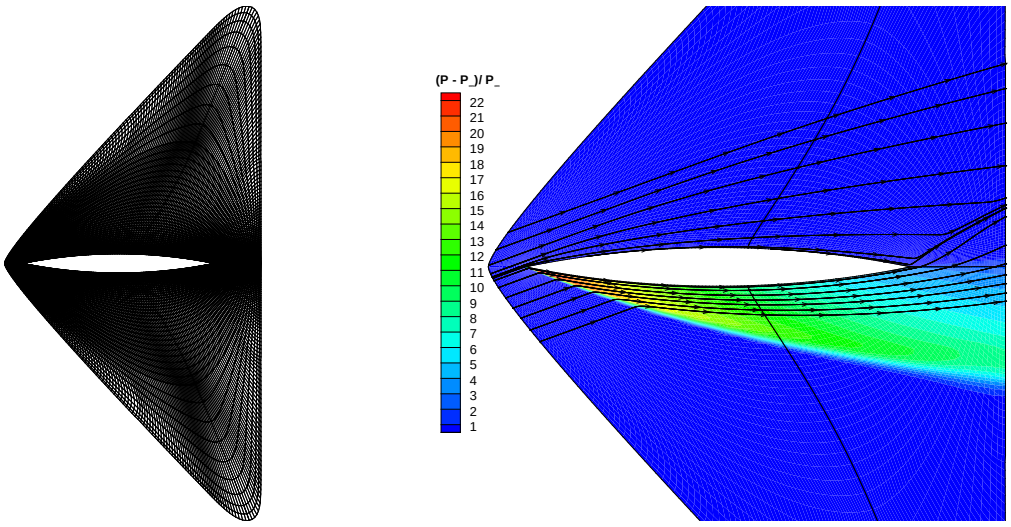

(a) Euler grid around airfoil (b) Pressure contours with streamlines at aoa = 20°

Figure 3: Euler grid, pressure contours on 10% thick bi-convex airfoil at free-stream Mach number of 6.86 and 20° angle of attack

the experimental results with in 4% error and Euler CFD results with in 5.4% error. Euler CFD results slightly overpredicted, when compared to experimental ones.

Table 1: Comparison of C_p for different cone semi-vertex angles at $M_{\infty} = 2.72$ and $Re = 5.5X10^5$

Cone semi-vertex angle (Deg.)	Experimental	Shock-expansion	Euler CFD
10	0.09526	0.09089	0.09615
15	0.18091	0.17862	0.18565
20	0.29523	0.29169	0.30055

3.2.2 Tangent-ogive cylinder with fineness ration of 3

Tangent-ogive cylinder with fineness ration of 3 and ogive radius of 9.25 times the diameter of cylinder is considered to test the tool at free-stream Mach numbers of 3, 4.25, 5.05 and 6.3. Figure 7(a) shows the Euler grid used for inviscid CFD analysis and figure 7(b) shows pressure contours with streamlines on tangent-ogive at free-stream Mach number of 6.3. Experimental results of Eggers et al [12] were used for comparison, which were conducted at NASA Ames supersonic wind tunnel at Reynolds numbers of $1.09X10^6$ at Mach numbers 3 and 4.25, $0.52X10^6$ at Mach number 5.05 and $0.22X10^6$ at Mach number 6.3. Figure 7(c) to (f) shows the comparison of C_p between shock-expansion, experimental and Euler CFD results at the free-stream Mach numbers considered. There is good agreement between experimental and Euler CFD results at almost all Mach numbers, where as shock-expansion results underpredicted at all Mach numbers. The deviation decreased with increasing Mach number.

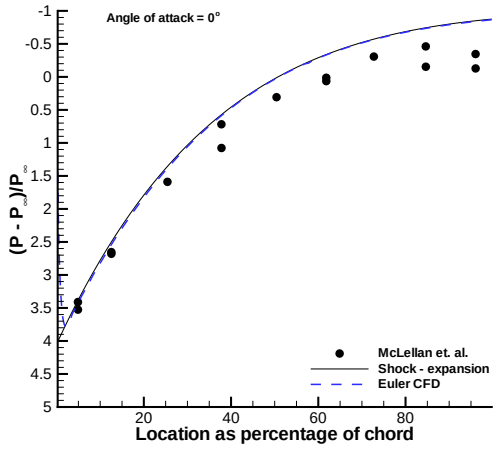

(a) Pressure distribution at aoa = 0°

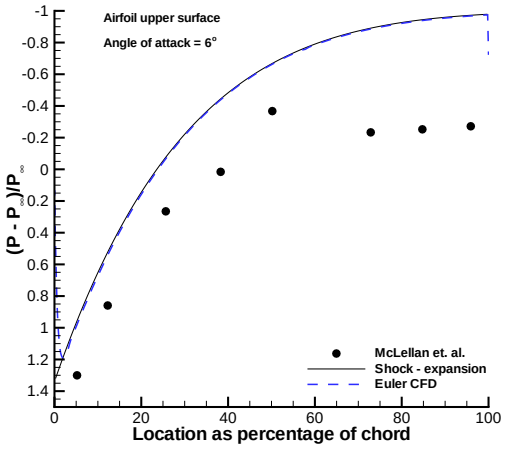

(b) Upper surface pressure distribution at aoa = 6°

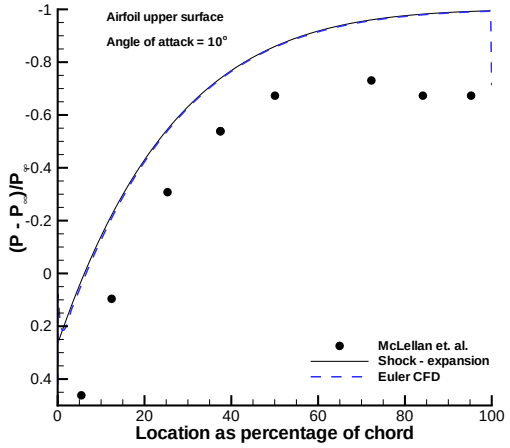

(c) Upper surface pressure distribution at aoa = 10°

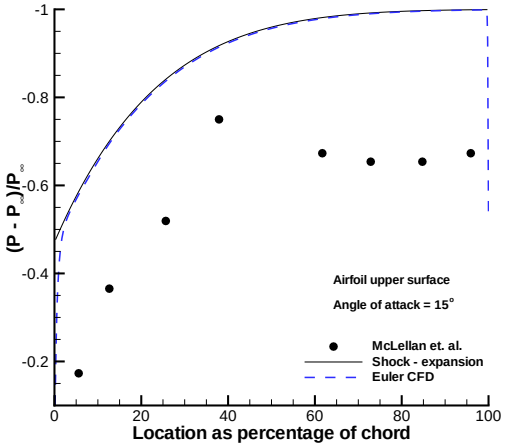

(d) Upper surface pressure distribution at aoa = 15°

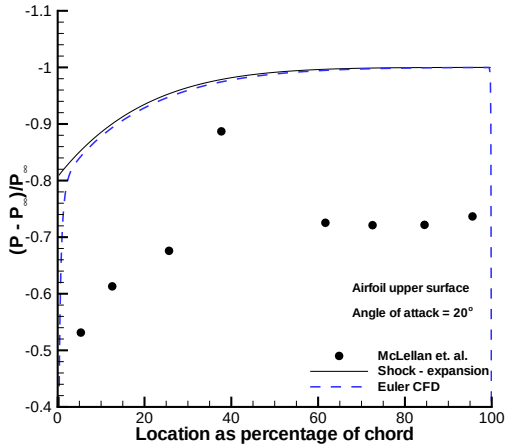

(e) Upper surface pressure distribution at aoa = 20°

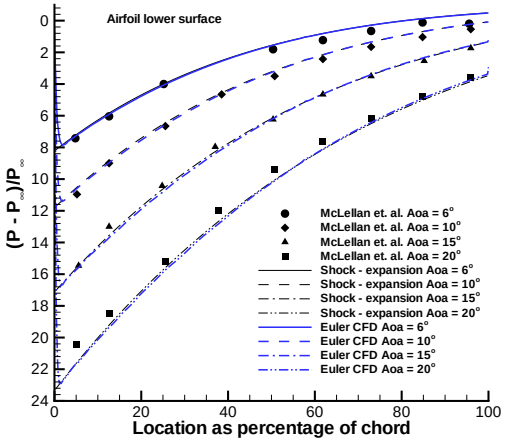

(f) Lower surface pressure distribution

Figure 4: Pressure distribution on 10% thick bi-convex airfoil at free-stream Mach number of 6.86 and different angle of attacks

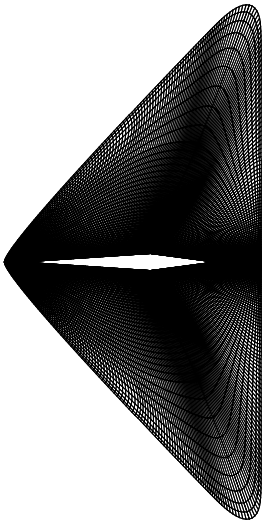

(a) Euler grid around all-body hypersonic aircraft

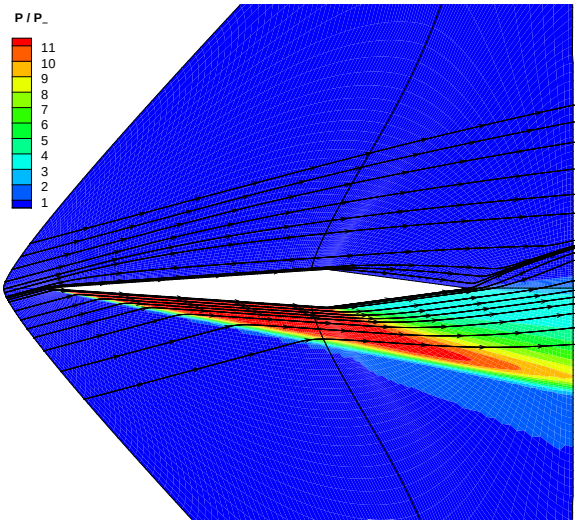

(b) Pressure contours with streamlines at aoa = 15°

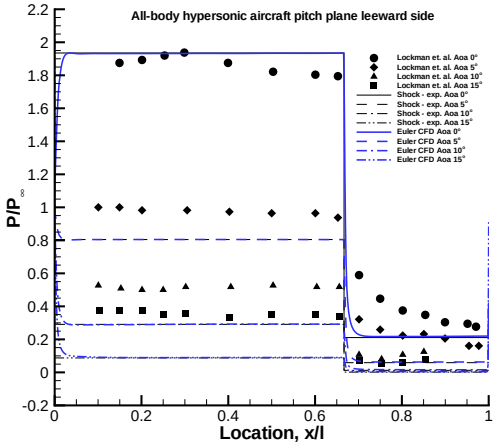

(c) Pressure distribution on upper surface

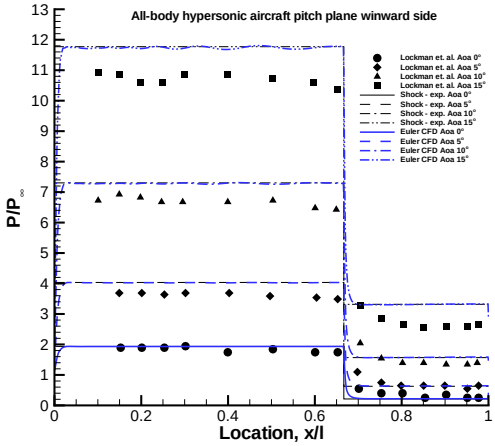

(d) Pressure distribution on lower surface

Figure 5: Euler grid, pressure contours and pressure distribution on all-body hypersonic aircraft at free-stream Mach number of 7.4 and different angle of attacks

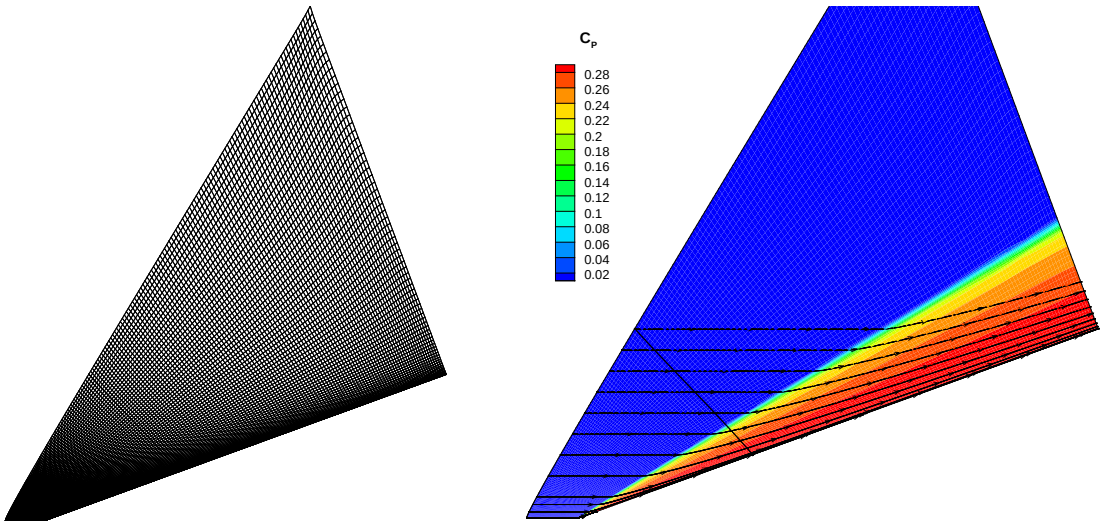

(a) Euler grid on cone (b) Pressure contours with streamlines on 20° cone

Figure 6: Euler grid, pressure contours on right circular cone with semi-vertex angle of 20° at a free-stream Mach number of 2.72

3.2.3 Cone-cylinder-flare configuration

Cone-cylinder-flare configuration is considered to test the tool at free-stream Mach numbers of 1.75, 2, 3, 4 and 4.5. Figure 8(a) shows the Euler grid used for inviscid CFD analysis and figure 8(b) shows pressure contours with streamlines on the configuration at free-stream Mach number of 4.5. Experimental results of Washington et al [13] were used for comparison, which were conducted at supersonic wind tunnel at Aberdeen, Maryland at Reynolds number of about $0.45X10^6$. Figure 8(c) to (f) shows the comparison of C_p between shock-expansion, experimental and Euler CFD results at the free-stream Mach numbers considered. There is good agreement between experimental and Euler CFD results at almost all Mach numbers. The shock-expansion results deviated more from CFD and experimental results at all Mach numbers on cylinder and flare sections, which can be attributed to neglected interaction of outward-running Mach waves with inward-running Mach waves from the shock and stream lines. This interaction reduces with increasing Mach number and hence the deviation decreased with increasing Mach number.

4 Conclusion

In the present study Shock-Expansion tool was developed and applied to three 2-D bodies at different angle of attacks and three axisymmetric bodies at zero angle of incidence for different Mach numbers. In all the cases, the results obtained are very much in good agreement with Euler CFD results, except for cone-cylinder-flare configuration, which can be attributed to influence of reflection Mach waves. In all the cases, the trends of experimental results were predicted. The time taken by shock-expansion calculations is very negligible, when compared with Euler CFD simulations. Moreover shock-expansion calculation doesn't need any grid, which saves grid generation time too. Hence quick inviscid estimates can be generated with reasonable accuracy. The deviation between the results of 2-D bodies and their corresponding experimental results increased with increase of angle of attack. These deviations can be attributed to increasing viscous effects with angle of attack on suction side, like separation. There is

better agreement on pressure side even at high angle of attacks. For axisymmetric case the accuracy of prediction increased with free-stream mach number.

Acknowledgments
This work has been supported by the Council of Scientific and Industrial Research, India. Thanks are due to Mr. Vajjala Keshava Suman, Scientist, CTFD Division, CSIR-NAL for helpful discussions throughout this work.

References

[1] Anderson, John David, Hypersonic and high temperature gas dynamics, McGraw-Hill series in Aeronautical and Aerospace Engineering, 1989.

[2] Maurice Rasmussen, Hypersonic flow, John Wiley & Sons, Inc., New York, 1994.

[3] Epstein, S. Paul, On the Air Resistance of Projectiles, Proc Natl. Acad. Sci. USA, 17(9), 532547, Sep 1931.

[4] Eggers, A. J., Syvertson, C. A., and Kraus, S., A Study of Inviscid Flow About Airfoils at High Supersonic Speeds, NACA Report 1123,1953.

[5] Syvertson, C. A., and Dennis, D. H., A Second-Order Shock Expansion Method Applicable t Bodies of Revolution Near Zero Lift, NACA TR 1323,1957.

[6] Jackson, C. M., Sawyer, W C., and Smith, R. S., A Method for Determining Surface Pressures on Blunt Bodies of Revolution at Small Angles of Attack in Supersonic Flow, NASA TN P-4865,1968.

[7] Dejarnette, F. K., and Ford, C. P., A New Method for Calculating Surface Pressures-on Bodies at an Angle of Attack in Supersonic Flow, Proceedings of the 11th Navy' Symposium on Aerobaffistics, Vol. 11, August 22-24, 1978, pp. 199-231.

[8] Moore, Frank G., Armistead, Michael A., Rowles, Steve H., and Dejarnette Fred K., Second-order Shock-Expansion Theory Extended to Include Real Gas Effects, NAVSWCTR 90-683, 1992.

[9] McLellan, Charles H., Bertram, Mitchel H., and Moore, John A., An Investigation of Four Wings of Square Plan Form at a Mach number of 6.86 in the Langley 11-Inch Hypersonic Tunnel, NACA RM L51D17,1951.

[10] Lockman, William K., Lawrence, Scott L., Cleary, Joseph W., Experimental and Computational Surface Flow-Field Results for an All-Body Hypersonic Aircraft, AIAA paper No. 90-3067, 1990.

[11] Yahalom Rafael, An Experimental Investigation of Supersonic Flow Past Yawed cones, Report No. AS-71-2, College of Engineering, University of California, Berkeley, 1971.

[12] Eggers, A. J. Jr., and Savin, Raymond C., A Unified Two-Dimensional Approach to the Calculation of Three-Dimensional Hypersonic Flows, With Application to Bodies of Revolution, NACA Report 1249, 1952.

[13] Washington, William D., and Humphery, James A., Pressure Measurements on Four Cone-Cylinder-Flare Configurations at Supersonic Speeds, AD 699359, 1969.

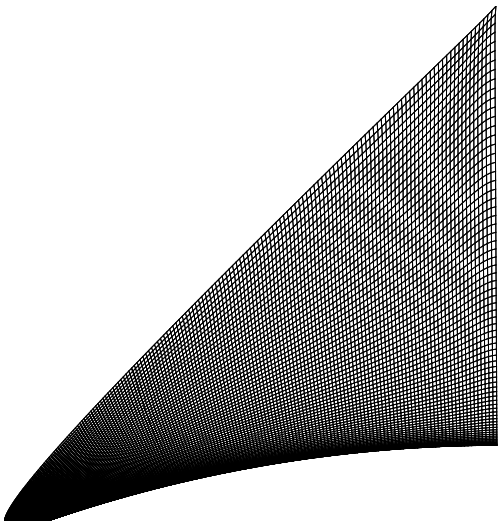

(a) Euler grid on tangent-ogive

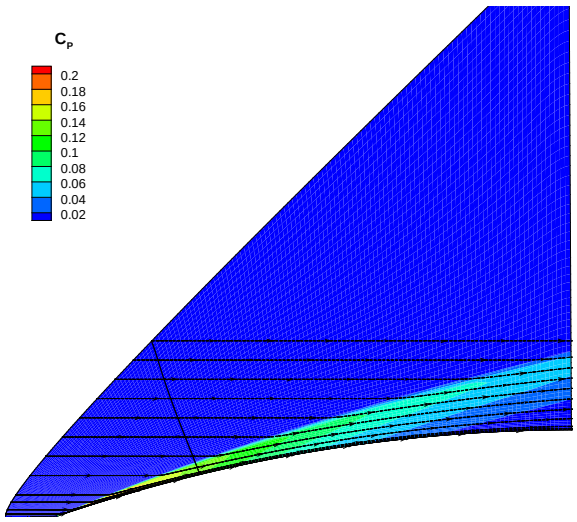

(b) Pressure contours with streamlines at Mach = 6.3

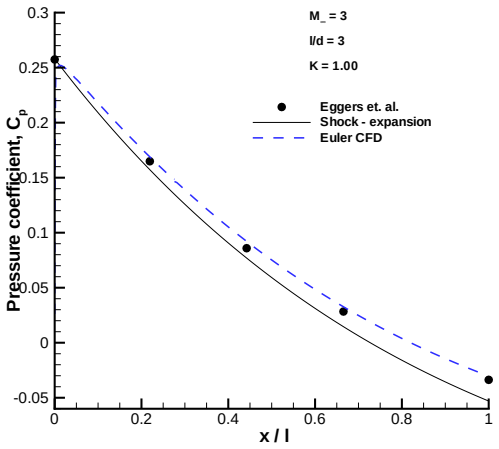

(c) C_p distribution at Mach = 3

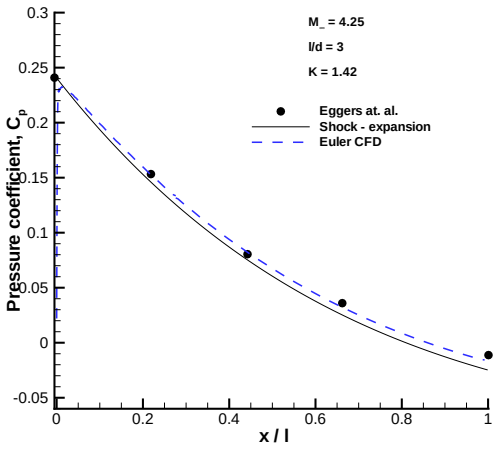

(d) C_p distribution at Mach = 4.25

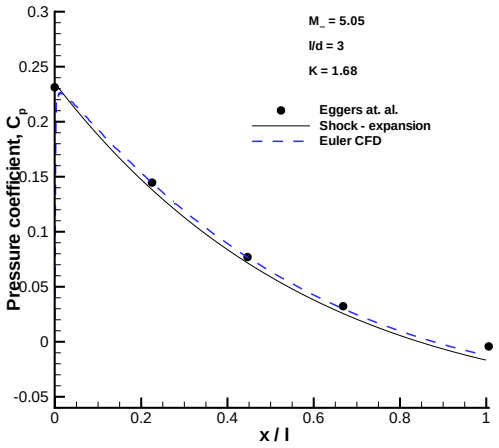

(e) C_p distribution at Mach = 5.05

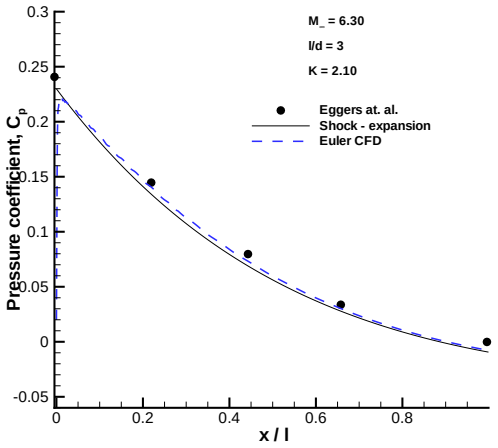

(f) C_p distribution at Mach = 6.3

Figure 7: Euler grid, pressure contours and C_p distribution on tangent-ogive cylinder with fineness ratio of 3 at different free-stream Mach numbers

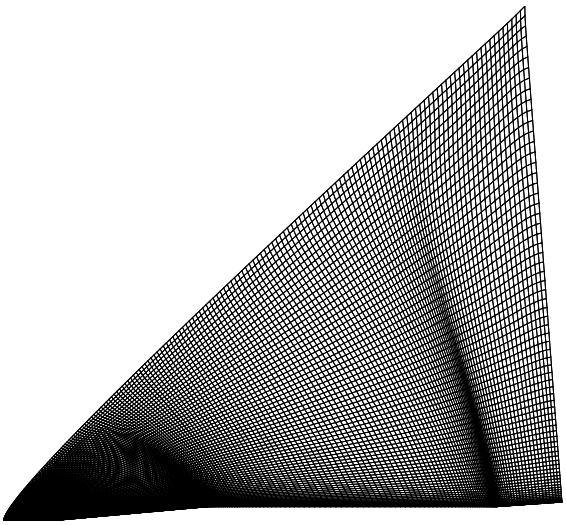

(a) Euler grid on cone-cylinder-flare

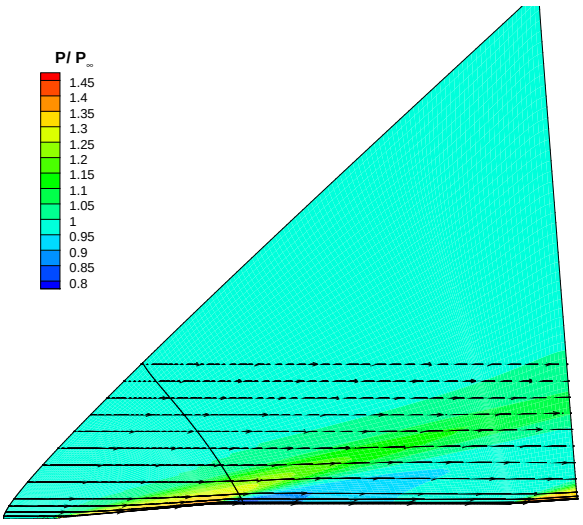

(b) Pressure contours with streamlines at Mach = 4.5

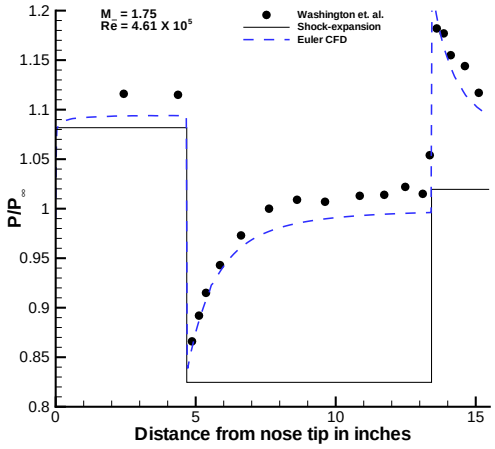

(c) Pressure distribution at Mach = 1.75

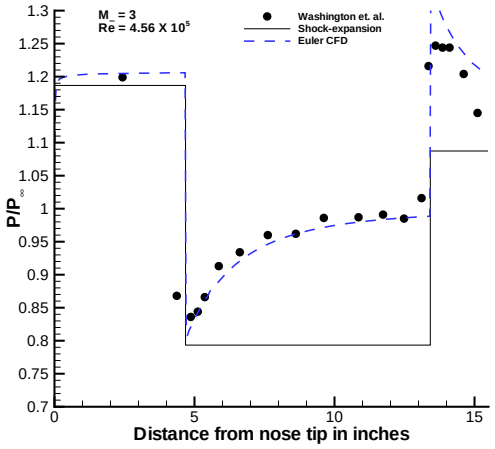

(d) Pressure distribution at Mach = 3

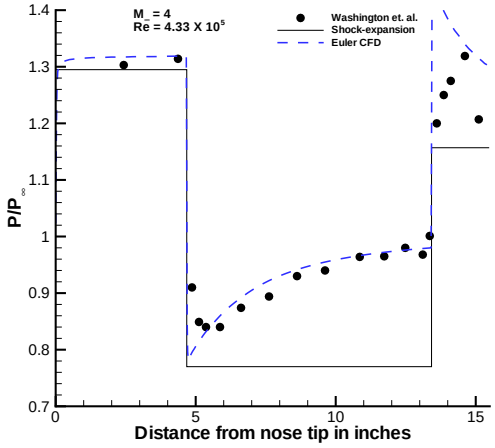

(e) Pressure distribution at Mach = 4

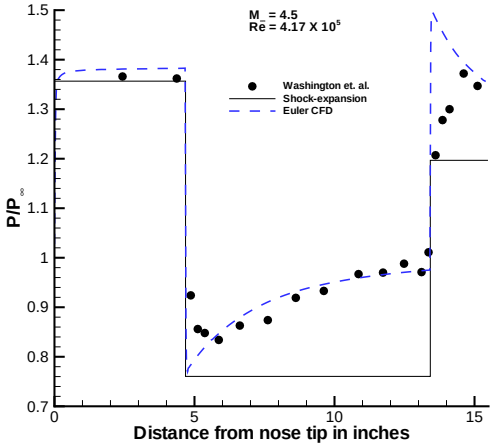

(f) Pressure distribution at Mach = 4.5

Figure 8: Euler grid, pressure contours and pressure distribution on cone-cylinder-flare configuration at different free-stream Mach numbers